6a

PNL-3497
UC-48

Interim Report

Environmental Radiation Safety: Source Term Modification by Soil Aerosols

O. R. Moss
M. D. Allen
E. J. Rossignol
W. C. Cannon

August 1980

Prepared for
Office of Advanced Nuclear Systems and Projects
Space and Terrestrial Systems Division
for the U.S. Department of Energy
under Contract DE-AC06-76RLO 1830

Pacific Northwest Laboratory
Operated for the U.S. Department of Energy
by Battelle Memorial Institute

Battelle

PNL-3497

PACIFIC NORTHWEST LABORATORY
operated by
BATTELLE
for the
UNITED STATES DEPARTMENT OF ENERGY
Under Contract DE-AC06-76RLO 1830

Printed in the United States of America
Available from
National Technical Information Service
United States Department of Commerce
5285 Port Royal Road
Springfield, Virginia 22151

Price: Printed Copy $_____*; Microfiche $3.00

*Pages	NTIS Selling Price
001-025	$4.00
026-050	$4.50
051-075	$5.25
076-100	$6.00
101-125	$6.50
126-150	$7.25
151-175	$8.00
176-200	$9.00
201-225	$9.25
226-250	$9.50
251-275	$10.75
276-300	$11.00

PNL-3497
UC-48

ENVIRONMENTAL RADIATION SAFETY: SOURCE TERM MODIFICATION BY SOIL AEROSOLS

Interim Report to
Office of Advanced Nuclear Systems and
Projects
Space and Terrestrial Systems Division

O. R. Moss
M. D. Allen
E. J. Rossignol
W. C. Cannon

August 1980

This report is based on work performed under
U.S. DOE Contract No. DE-AC06-76RLO 1830

Pacific Northwest Laboratory
Richland, Washington 99352

CONTENTS

TABLES

FIGURES

FIGURES (continued)

INTRODUCTION

BACKGROUND

The goal of this project is to provide information useful in estimating hazards related to the use of a pure refractory oxide of ^{238}Pu as a power source in some of the space vehicles to be launched during the next few years. Although the sources are designed and built to withstand re-entry into the earth's atmosphere, and to impact with the earth's surface without releasing any plutonium, the possibility that such an event might produce aerosols composed of soil and $^{238}PuO_2$ cannot be absolutely excluded.

This report presents the results of our most recent efforts to measure the degree to which the plutonium aerosol "source term" might be modified in a terrestrial environment. The five experiments described represent our best effort to use the original experimental design[1] to study the change in the size distribution and concentration of a $^{238}PuO_2$ aerosol due to coagulation with an aerosol of clay or sandy loam soil.

The impact of a falling projectile on soil may produce an annulus of fluidized dust surrounding the object. It is important to be able to estimate the soil particle concentration within the dust cloud, and its duration, because any major change in the particle size distribution and concentration of respirable PuO_2 aerosol leaking from the object would be expected to occur within the annulus of dust. The literature on terradynamics, the study of the formation of craters in soil, contains very little information on the aerosol produced by the impact. However, some information is provided on the depth of penetration, crater diameter, projectile diameter, and kinetic energy.[2] From a review of this literature, it is assumed that the volume of the aerosol cloud formed around a 30-cm-dia., spherical projectile is 1 liter. (This corresponds to a height of 4 cm and a thickness of 2 cm.)

Changes in the respirable PuO_2 aerosol size distribution or concentration in the first few minutes following impact will be due primarily to coagulation. Three types of particle motion that cause coagulation must be considered: Brownian motion, turbulence, and scavenging by large, sedimenting particles. In the dust cloud formed by the impact, the concentration of soil particles will initially be high and the dominant coagulation mechanisms will be Brownian and turbulent motion. The dust cloud will be diluted in a few seconds by atmospheric motion so that Brownian and turbulent coagulation will no longer be important. After a few seconds, scavenging by large soil particles falling under the influence of gravity may become the dominant particle removal mechanism.

The coagulation rate of the aerosol released into the annulus by the impact can be calculated if the particle concentration and size are estimated. In the Overall Safety Manual,[3] the ^{238}Pu activity released by impact onto granite is estimated to be 252.4 Ci. The size distribution of the released material is assumed to be the same as the size distribution of the fractured fuel, which is shown in Figure 1.[3-5] The particle size distribution can be separated into a log-normal distribution of large particles comprising 80% of the mass (MMD = 1040 μm, GSD = 1.74), and a log-normal distribution of small particles comprising 20% of the mass (MMD = 55 μm, GSD = 4.1). Here, MMD represents the mass median diameter and GSD represents the geometric standard deviation.

The diameter of the particle of average volume, $\bar{D}_v$, is given[6] by

$$\bar{D}_v = \text{MMD} \exp[-1.5 (\ln \text{GSD})^2].$$

The total number of particles released, N, is calculated by dividing the total volume of material released by the volume of a single particle having diameter $\bar{D}_v$.

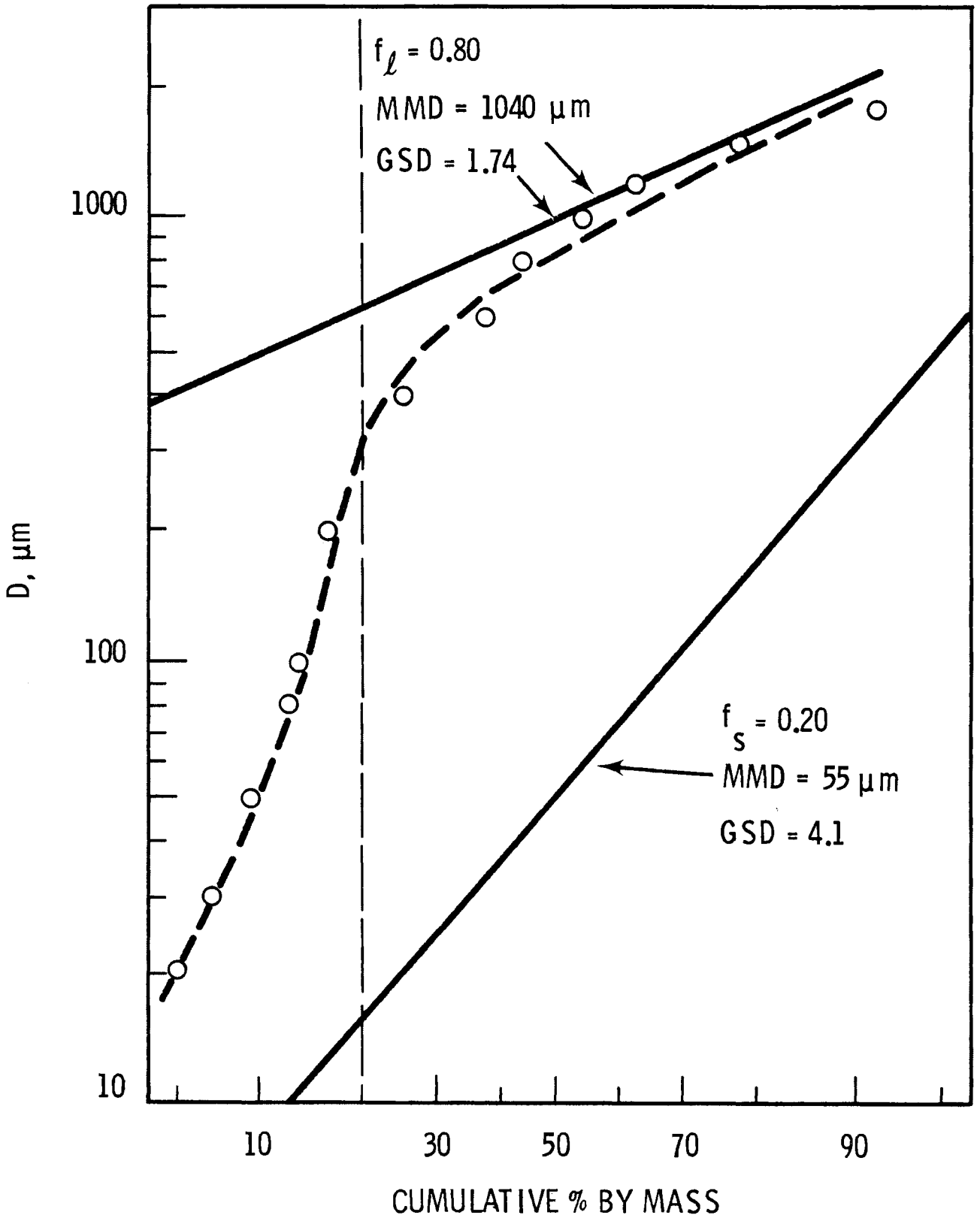

FIGURE 1. Size Distribution of $^{238}PuO_2$ Fractured Fuel

$$N = \frac{6A}{S_p \rho \pi \bar{D}_v^3}, \qquad (1)$$

where A = activity released, S_p = specific activity (13.85 Ci/g for $^{238}PuO_2$), and ρ = density (11.5 g/cm^3 for $^{238}PuO_2$). The large mass fraction of the released fuel accounts for 1.07×10^4 particles; the small mass fraction accounts for 1.60×10^{11} particles. The initial concentration of released fuel in the 1-liter annulus is approximately 1.6×10^8 particles/cm^3.

The five experiments reported here investigate the changes that may occur in the respirable PuO_2 aerosol due to coagulation by scavenging of large soil particles falling under the influence of gravity. This process should be the dominant particle removal process occurring in the period between a few seconds and a few minutes following impact. However, the primary changes in the source term are believed to be due to Brownian and turbulent coagulation. For this reason, a theoretical model is included in the following section which predicts the decrease in the respirable PuO_2 particle concentration due to coagulation in the first few seconds following impact.

THEORETICAL MODEL

In order to estimate the possible reduction in the source term due to coagulation, it is necessary to consider the aerosol produced by the impact of a radioisotope thermoelectric generator (RTG) on soil. It is assumed that the concentration of nonrespirable soil particles in a turbulently mixed annulus surrounding the projectile is initially 10^{10} particles/cm^3. The concentration of soil aerosol may be orders of magnitude higher, but this model is intended to be conservative. The particle size is not required in this model, but it is assumed that all of the soil particles have an aerodynamic diameter greater

than 4 μm. The respirable fraction of PuO_2 aerosol consists of particles with aerodynamic diameters less than 4 μm and can be estimated[5,7] to be 0.0058 times the initial concentration of released fuel. The initial concentration of PuO_2 aerosol was estimated (in the Introduction) to be 1.6×10^8 particles/cm^3, so the respirable fraction of PuO_2 aerosol is approximately $0.0058 \times 1.6 \times 10^8 \simeq 10^6$ particles/cm^3.

Coagulation of particles can be the result of three mechanisms: Brownian motion, sedimentation (e.g., the scavenging of particles by raindrops), and turbulence (mainly affecting the coagulation of particles larger than 1 μm).[8-12] In the short term, coagulation by sedimentation should have little influence on reducing particle concentration, especially if the mixing caused by the impact is so violent that there is no settling of particles.[9,11] Coagulation of particles will be dominated by turbulent and Brownian motion in the short term. A conservative estimate of the coagulation rate is obtained by ignoring turbulent motion and taking Brownian coagulation as the only mechanism. Electrical charge[12] and polydispersity[10,11] can affect the coagulation rate, but the effects are assumed to be minor and are therefore neglected in this model.

The initial particle concentration, N_o, in the annulus surrounding the projectile following impact is the sum of the soil and PuO_2 particle concentrations, i.e., $10^{10} + 10^6 \simeq 10^{10}$ particles/cm^3. The total particle concentration, N (t), remaining after time t is given by

$$N(t) = \frac{N_o}{1 + \frac{t}{\tau}} \qquad (2)$$

for a monodisperse aerosol undergoing Brownian coagulation.[8,13,14] In this equation, τ is the coagulation half-time and is given by

$$\tau = 2/K_c N_o.$$

Here, K_c is the coagulation coefficient and is given by $K_c = 6 \times 10^{-10} C(D)$, where C(D) is the slip correction factor. In the assumed aerosol, 99.99% of the particles have an aerodynamic diameter (D_{ae}) greater than 4 μm and, for particles with D_{ae} greater than 4 μm, C(D) can be taken as equal to 1. Equation (2) gives the total particle concentration at any time t, regardless of whether the particles are singlets, doublets, triplets, or aggregates of many primary particles.

Equations have also been derived to calculate the number of singlets, doublets, or, in general, the number of aggregates consisting of κ primary particles existing at any time t.[14] The number of singlets, N_1, existing at any time t is given by

$$N_1 = \frac{N_o}{\left(1 + \frac{t}{\tau}\right)^2} \tag{3}$$

and the number of doublets, N_2, existing at any time t is given by

$$N_2 = \frac{\frac{N_o t}{\tau}}{\left(1 + \frac{t}{\tau}\right)^3} \tag{4}$$

In general, the number of aggregates which consist of κ primary particles existing at any time t is given by

$$N_\kappa = \frac{N_o \left(\frac{t}{\tau}\right)^{\kappa - 1}}{\left(1 + \frac{t}{\tau}\right)^{\kappa + 1}} \tag{5}$$

For an initial particle concentration of 10^{10} particles/cm^3, the coagulation half-time τ is 0.33 sec. The initial concentration of respirable PuO_2 particles will also be reduced by half in 0.33 sec.

In this model, a single collision between a respirable PuO_2 particle and a nonrespirable soil particle will remove the PuO_2 particle from the respirable fraction. The dublet formed by the collision between a particle with D_{ae} less than 4 μm and a particle with D_{ae} greater than 4 μm will have an aerodynamic diameter greater than 4 μm and, therefore, will be nonrespirable. Since soil particles make up 99.99% of the number concentration, it is assumed that each collision of a PuO_2 particle is with a soil particle.

Just after impact of the RTG on soil at time t = 0, there are 10^6 respirable PuO_2 particles/cm^3 mixed with a soil aerosol of 10^{10} particles/cm^3. As the respirable PuO_2 particles coagulate with nonrespirable soil particles to form doublets, triplets, and aggregates composed of many primary particles, they are removed from the respirable fraction; only the singlet PuO_2 particles remain respirable. The number of singlets, N_1, remaining as a function of time t can be calculated using Eq. (3); this has been done and the results are plotted in Figure 2. At t = 0, $N_1 = 10^6$ particles/cm^3. After 3 sec, N_1 has decreased to 10^4 particles/cm^3 for $\tau = 0.33$ sec. It is assumed that after 3 sec the 1-liter annulus of dust formed around the projectile by the impact will be sufficiently diluted by atmospheric motion to reduce the particle concentration enough so that Brownian coagulation is no longer the dominant mechanism. After 3 sec, scavenging of respirable PuO_2 particles by sedimentation of large, nonrespirable soil particles may become the dominant removal mechanism.

The total number of respirable PuO_2 particles after 3 sec is estimated using this physical model to be 10^4 particles/cm^3 x 10^3 cm^3, or 10^7 particles. These respirable PuO_2 particles may also be removed from the atmosphere by other particle removal processes, such as scavenging and turbulent deposition.

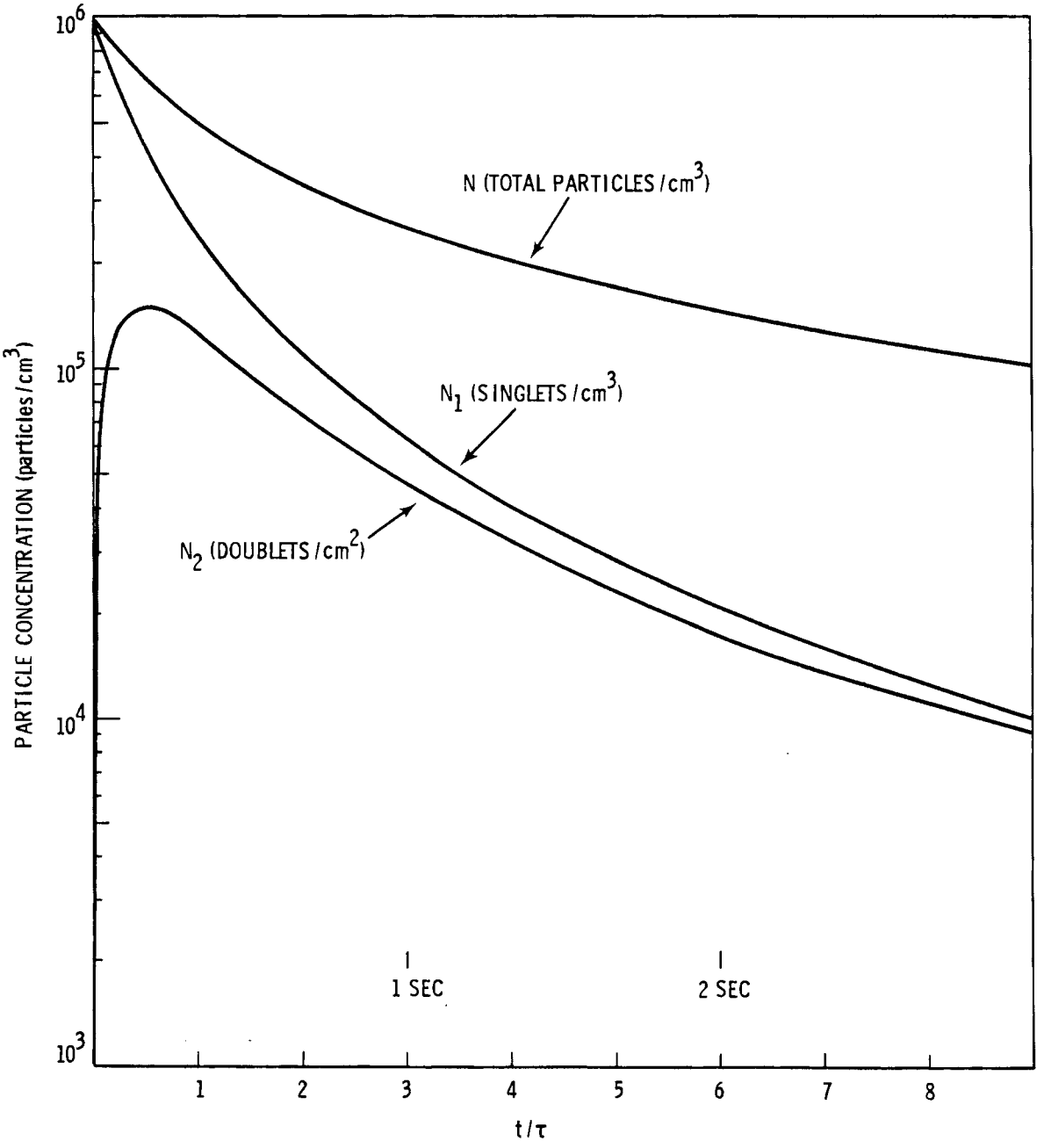

FIGURE 2. Respirable Particle Concentration vs. Time (for τ = 0.33)

This model is independent of particle size and gives a conservative estimate of the reduction in the respirable fraction of PuO_2 due to Brownian coagulation. The model is applicable provided the concentration of soil particles with D_{ae} greater than 4 μm is at least 10^{10} particles/cm^3. If the particle size of the respirable PuO_2 is significantly less than 1 μm, then the slip correction factor is important and the coagulation rate will be even higher.

EXPERIMENTAL MODEL

Mixing of soil and plutonium aerosols was carried out in the only available facility. This low-speed wind tunnel was designed to study plutonium uptake in plants from foliar deposition.[15,16]

The experimental procedure consisted of generating aerosols through a mixing nozzle and measuring the total deposition, airborne concentration, and particle size distribution. The size distributions were measured by three methods: autoradiography (AR), electron microscopy (EM), and cascade impactors. A Wright dust feed mechanism (WDF) was used for aerosol generation of the soil,[17] and a Retec nebulizer (RETEC Development Laboratory, Portland, OR) for the plutonium dioxide (Figure 3). These five experiments demonstrate that for initial concentrations of 0.6 to 2.5 x 10^6 particles/cm^3 (soil and plutonium dioxide, respectively), the presence of soil aerosol causes a change in the airborne source term. The following changes were observed:

- total activity concentration decreased by 5%;
- particle count decreased by 65 and 49%;
- the spread in the particle size distribution decreased;
- no significant change was seen in the respirable fraction.

The changes observed show the influence of particle scavenging due to sedimentation of soil particles through a cloud of PuO_2 aerosol having a

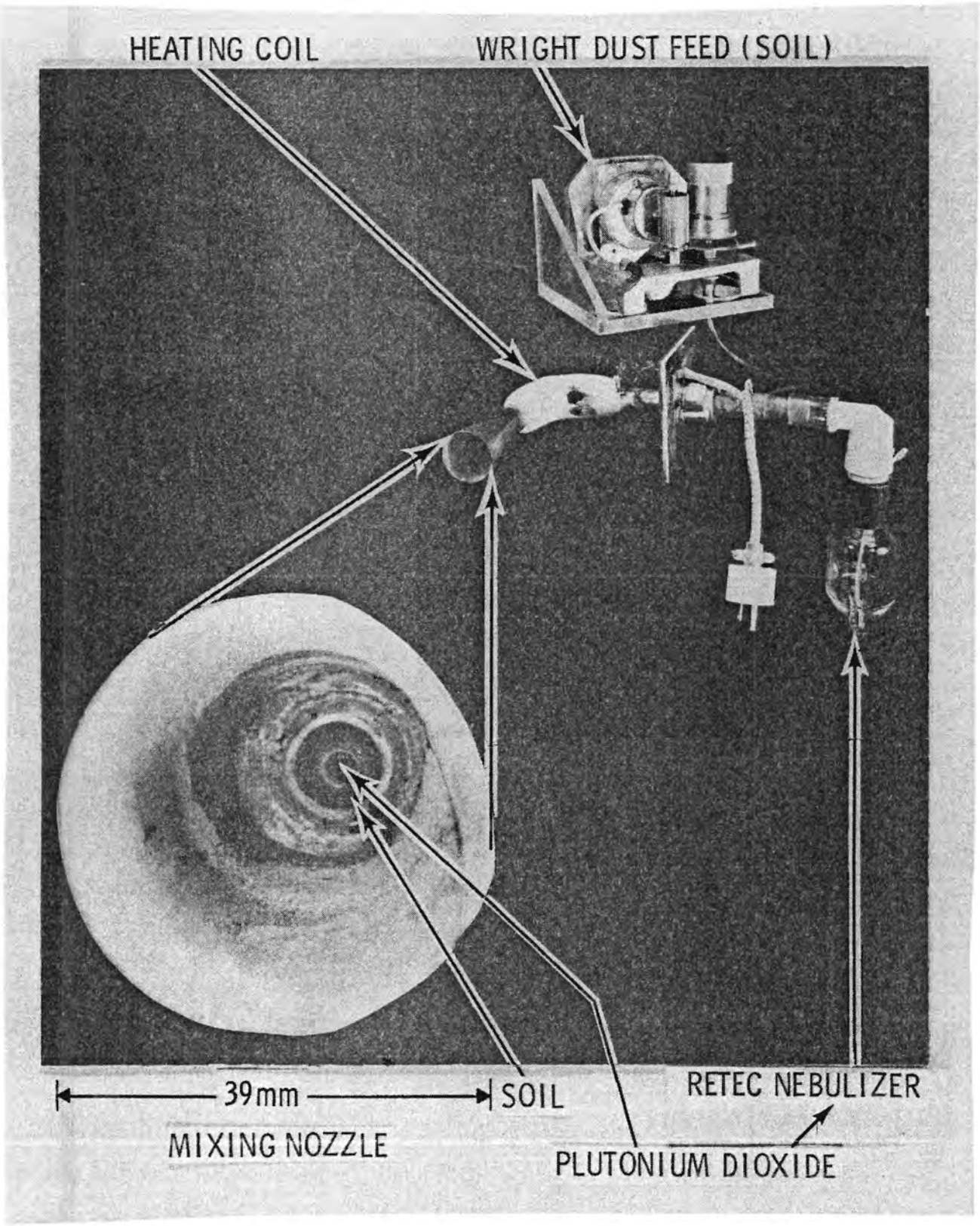

FIGURE 3. Aerosol Generation System

relatively low concentration. However, the major changes expected to occur in the source term produced by impact on soil would be due to Brownian and turbulent coagulation. These changes were not tested in these experiments since the initial concentrations were too low to cause significant Brownian coagulation.

MATERIALS AND METHODS

Powders of pure plutonium oxide, sandy loam soil and clay soil were used in this experiment. The $^{238}PuO_2$ powder was sieved to a maximum particle size of 10 μm at Los Alamos Scientific Laboratories before shipment to the Pacific Northwest Laboratory in 1974. The sandy loam soil was a sample of the volcanic tuft underneath Los Alamos, NM. The clay soil was obtained from stream beds in the valley below Los Alamos. The mass median diameters and geometric standard deviations of the sandy loam soil and clay soil were measured by sedimentation and sieving.[18] The mass median diameters were 57 μm and 1.1 μm, with geometric standard deviations of 4.4 and 6.0, respectively. The soils were stored dry.

THE WIND TUNNEL

The low-speed wind tunnel available for this study was built for a study of plutonium uptake into plants from foliar deposition.[15,16] The tunnel, constructed of stainless steel, is 178 cm long; the inlet end has a square cross-section, 20.3 cm on each side; the center section is 30.5 cm on each side. The transition between the two sections of the tunnel is shown in Figure 4. Plants and equipment can be positioned through a file-cabinet-type drawer located in the center section of the tunnel.

To provide double containment, the entire wind tunnel is enclosed in a 2.4 x 0.8 x 0.8-m plexiglas glove box. In operation, a negative pressure differential exists between the glove box and the room as well as between the tunnel and the glove box.

The maximum air velocity in the tunnel is 30 cm/sec (i.e., less than 0.7 miles/hour, a very slow walk). For the five experiments reported here, the tunnel was operated at 0.9 cm/sec, a total airflow of 50 ℓ/min (1.8 cfm).

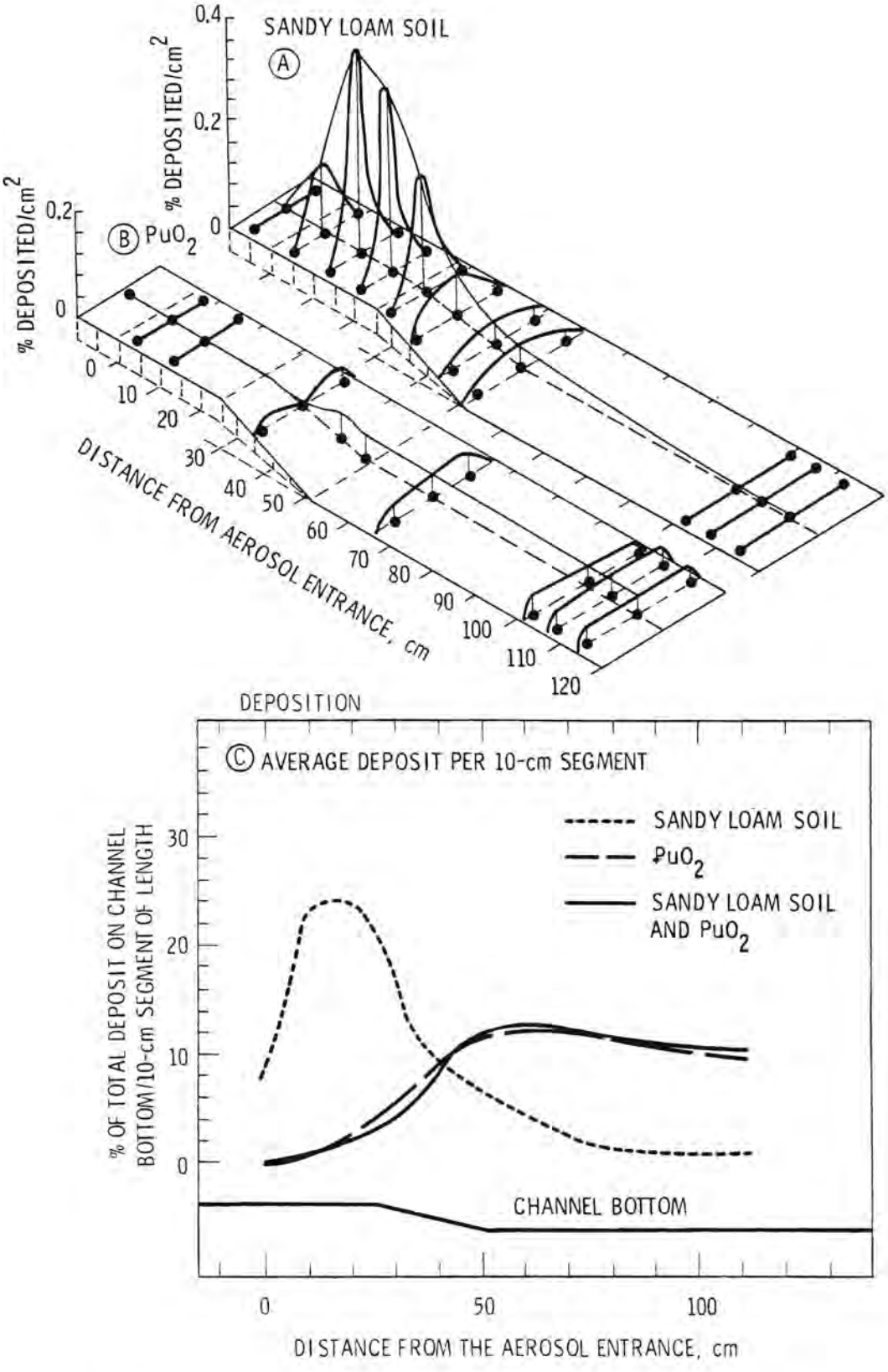

FIGURE 4. Filter Distribution Pattern of Deposited Activity

AEROSOL GENERATION

The $^{238}PuO_2$ aerosol was nebulized from an aqueous suspension with a Retec PN 7002 aerosol generator operated at 30 psi. The suspension consisted of the supernate drawn from a sedimentation flask such that all particles were less than 10 μm. Air was bubbled through the suspension. Total flow rate through the nebulizer was 10 ℓ/min.

The clay and sandy loam soils were aerosolized with the Wright dust feed (WDF) generator[17] at a gear ratio of 1:1. Total air flow through the WDF was 16 ℓ/min. Each soil passed through an 800-μm sieve before being packed into the WDF cup.

The aerosol generators fed into a mixing nozzle at the end of the wind tunnel. The plutonium aerosol entered along the axis of the nozzle; the soil aerosol entered through an annulus around the plutonium aerosol (Figure 3). The dimensions of the nozzle are given in previous reports.[18,19] At the point of first mixing, the diameter of the plutonium entry line is 0.32 cm; the diameter of a circle of area equal to the cross-sectional area of the soil annulus is 0.9 cm. The Reynolds numbers for the two flows are 4150 and 2350, respectively. At the exit of the nozzle, the Reynolds number for the total flow is 900.

SAMPLING: TOTAL MASS OR ACTIVITY DEPOSITED

The total mass of soil or the total activity of $^{238}PuO_2$ deposited on the wind-tunnel floor was estimated by measuring the mass or activity of material deposited on glass fiber filters placed on the channel floor. Examples of the filter distribution pattern are shown in Figure 4A. The amount of soil on each filter was weighed using an Ainsworth 24N balance. The amount of activity was measured by sealing the filters with transparent tape and counting the

gamma radiation with a NaI detector. Known $^{238}PuO_2$ sources were counted with each set of samples to check the calibration of the NaI detector.

SAMPLING: TOTAL MASS OR ACTIVITY AIRBORNE

Isokinetic filter-paper samples were taken at midchannel, 57, 81, 123 and 139 cm from the outlet of the aerosol mixing nozzle. Sample flow rates of 0.15 ℓ/min were drawn through 25-mm filters.

SAMPLES: PARTICLE SIZE, AMAD AND MMAD

The AMAD of the $^{238}PuO_2$ aerosol was measured with a Mercer cascade impactor (MCI), operated at 0.6 ℓ/min. The stages of the impactor were gamma-counted in the same manner as the filter samples. The MMAD of the soil aerosol was measured with an Andersen cascade impactor (ACI), operated at 18 ℓ/min. Each stage of the impactor was weighed. All impactor samples were taken approximately at midchannel, 88 cm from the end of the aerosol mixing nozzle. All MCI samples were taken isokinetically. The ACI samples were taken at as close to isokinetic conditions as possible. Only 23% of the total flow through this impactor was from the sampling nozzle; the rest was supplied by dilution air.[18]

SAMPLING: PARTICLE SIZE, D_p

The distribution of projected area diameters, D_p, was obtained from transmission electron microscope (TEM) photographs. The aerosol was collected on TEM carbon substrate grids with a PNL-built thermal precipitator similar to those described by Swift.[20] Projected area diameter distributions were measured with a Zeiss Particle Size Analyzer. Samples were collected approximately 98 cm from the end of the aerosol mixing nozzle.

SAMPLING: PARTICLE SIZE, AR SIZING

The size distribution of the plutonium dioxide particles was measured using autoradiography. A sample of the airborne dust was collected on a 25-mm filter positioned at midchannel, 57 cm from the end of the aerosol mixing nozzle. The filters, each containing no more than 2 nCi of activity, were sent to Dr. M. W. Nathans (LFE, Environmental Analysis Laboratories, 2030 Wright Avenue, Richmond, CA 94804) for autoradiographic analysis. Soil particles associated with plutonium dioxide particles were sized on selected filters. This was done by matching fields on the autoradiographic film and light microscope slide.

RESULTS

The experimental approach was to generate an aerosol of clay soil, sandy loam soil, or plutonium dioxide in the wind tunnel and measure the amount deposited and the amount airborne. Particle size distributions were also measured by cascade impactor, electron microscopy and, for $^{238}PuO_2$, autoradiography. The same measurements were then made on combined aerosols: $^{238}PuO_2$ with clay soil and $^{238}PuO_2$ with sandy loam soil. Except for the change in aerosol, all other conditions in the wind tunnel were kept as constant as possible for all experiments.

SAMPLING: TOTAL MASS OR ACTIVITY DEPOSITED

The total mass or activity deposited in the wind tunnel during each experimental run can be calculated from columns 3, 8 and 9 of Table 1. The deposition of dust along the length of the wind tunnel is shown in the set of curves marked "Deposition": Figure 5 for the clay soil and $^{238}PuO_2$ aerosols and Figure 6 for the sandy loam soil and $^{238}PuO_2$ aerosols. The amount of material deposited on each 10-cm section down the length of the wind tunnel was plotted as percent of the total amount deposited on the floor of the wind tunnel. The vertical lines represent the extremes; the curves represent the averages of two identical experiments, run one after the other (Table 1).

The amount of material deposited in the aerosol mixing nozzle was not used to calculate the deposition curves, but was included in the calculation of the total amount generated (column 3, Table 1). The total amount of material generated is split into three fractions: amount airborne at the end of the tunnel, amount deposited in the wind tunnel, and amount deposited in the

TABLE 1. Summation of the Three Single Aerosol and the Two Aerosol Interation Experiments

	COLUMN: AEROSOL	(1) GENERATION TIME, ΔT (min)	(2) INITIAL CONCENTRATION OF PuO_2 SOLUTION mCi/ml	(3) TOTAL AMOUNT GENERATED AIRBORNE + DEPOSIT (mCi)[a]	(4) ESTIMATED FROM GENERATOR OUTPUT (g)	(5) ESTIMATED FROM GENERATOR OUTPUT (mCi)	(6) MASS OF SOIL IN THE GENERATOR OUTLET (mg)	(7) AIRBORNE CONCENTRATION AT 110 cm (nCi/ℓ)[b]	(8) DISTRIBUTION % AIRBORNE	(9) % DEPOSITED	(10) % OTHER	(11) AEROSOL DISTRIBUTION SAMPLED AT 82 cm CRITICAL X^2 = 9.2 AMAD	(12) GSD	(13) ΣX^2
1.	CLAY SOIL	90	-----	4.7 g	5.8	-----	2520	189 μg/ℓ	17	29	54	2.9	2.2	26.4[c]
	CLAY SOIL	90	-----	5.0 g	5.8	-----	2620	146 μg/ℓ	13	34	53	2.8	2.3	19.1[c]
2.	SANDY LOAM SOIL	180	-----	13.0 g	12.7	-----	6467	59 μg/ℓ	4	45	51	4.1	2.5	28.6[c]
	SANDY LOAM SOIL	180	-----	12.3 g	12.7	-----	6548	58 μg/ℓ	4	42	54	4.1	2.4	18.5[c]
3.	238-PuO_2	20	1.84	1.12	-----	25.7	-----	943	84	15	1	2.2	2.5	8.8
	238-PuO_2	20	1.85	1.49	-----	20.1	-----	1156	78	17	5	2.0	2.5	7.7
4.	PuO_2 + CLAY SOIL	20	1.54	0.83	1.7	17.7	686	726	87	9	4	1.9	2.4	8.1
	PuO_2 + CLAY SOIL	20	1.68	0.82	1.7	18.5	716	800	91	8	1	2.3	2.2	11.6
5.	PuO_2 + SANDY LOAM SOIL	20	0.75	0.61	1.8	12.8	643	500	83	12	5	1.8	2.1	8.4
	PuO_2 + SANDY LOAM SOIL	20	0.71	0.64	1.8	8.9	1153	480	75	18	7	1.8	2.2	5.6

[a] UNIT IS mCi UNLESS OTHERWISE INDICATED

[b] UNIT IS nCi/ℓ UNLESS OTHERWISE INDICATED

[c] CRITICAL X^2 = 10.2

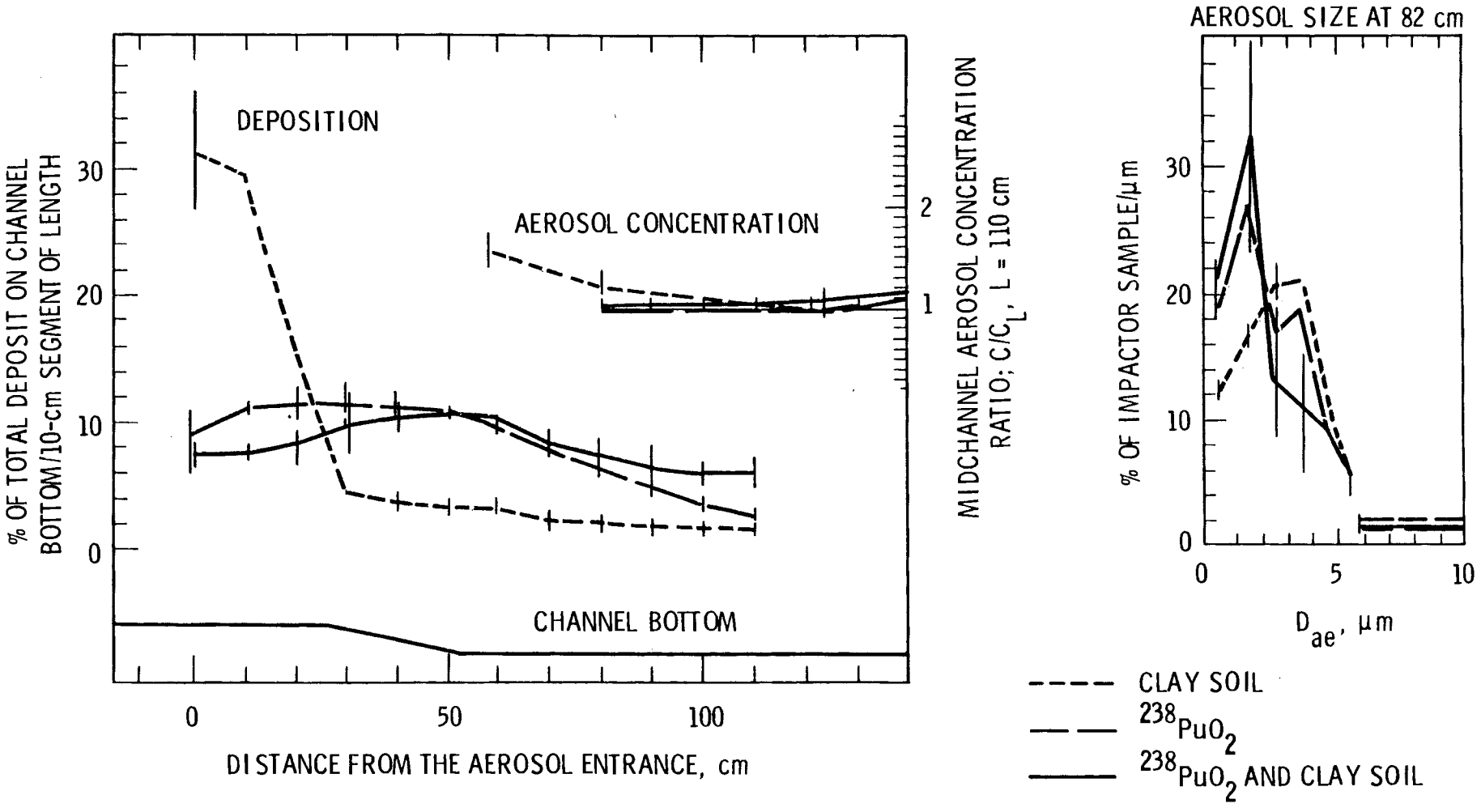

FIGURE 5. Deposition of Dust Along Length of Wind Tunnel for Clay Soil Plus $^{238}PuO_2$ Aerosols

aerosol mixing nozzle (Table 1, columns 8, 9 and 10). The total amount generated was also calculated by measuring the amount in the aerosol generators before and after each experiment. There was good agreement (Table 1) between the WDF output (column 4) and the total mass of dust generated, based on wind tunnel samples (column 3). The nebulizer output (column 5) is in poor agreement with the total generated activity given in column 3, possibly because of losses in the nebulizer.

SAMPLING: TOTAL MASS OR ACTIVITY AIRBORNE

The total mass or activity airborne at different midchannel distances from the aerosol inlet is shown for each dust in Figures 5 and 6. The y-axis is the ratio of the concentration, measured at any location, to the airborne concentration measured at 110 cm from the aerosol inlet. The latter concentration is listed in Table 1, column 7.

SAMPLING: PARTICLE SIZE, AMAD

The aerodynamic size distribution for each aerosol is listed in Columns 11 and 12, Table 1. The chi-square values (column 13) are a measure of how close the cascade impactor data fit a log-normal particle size distribution. The distribution is assumed not to be log-normal (0.1 level of significance) if the chi-square values are greater than 9.2 for Mercer or 10.6 for Andersen cascade impactors. A curve of the size distribution, averaged between the duplicate experimental runs, is included in Figure 5 for the clay soil and in Figure 6 for the sandy loam soil aerosols.

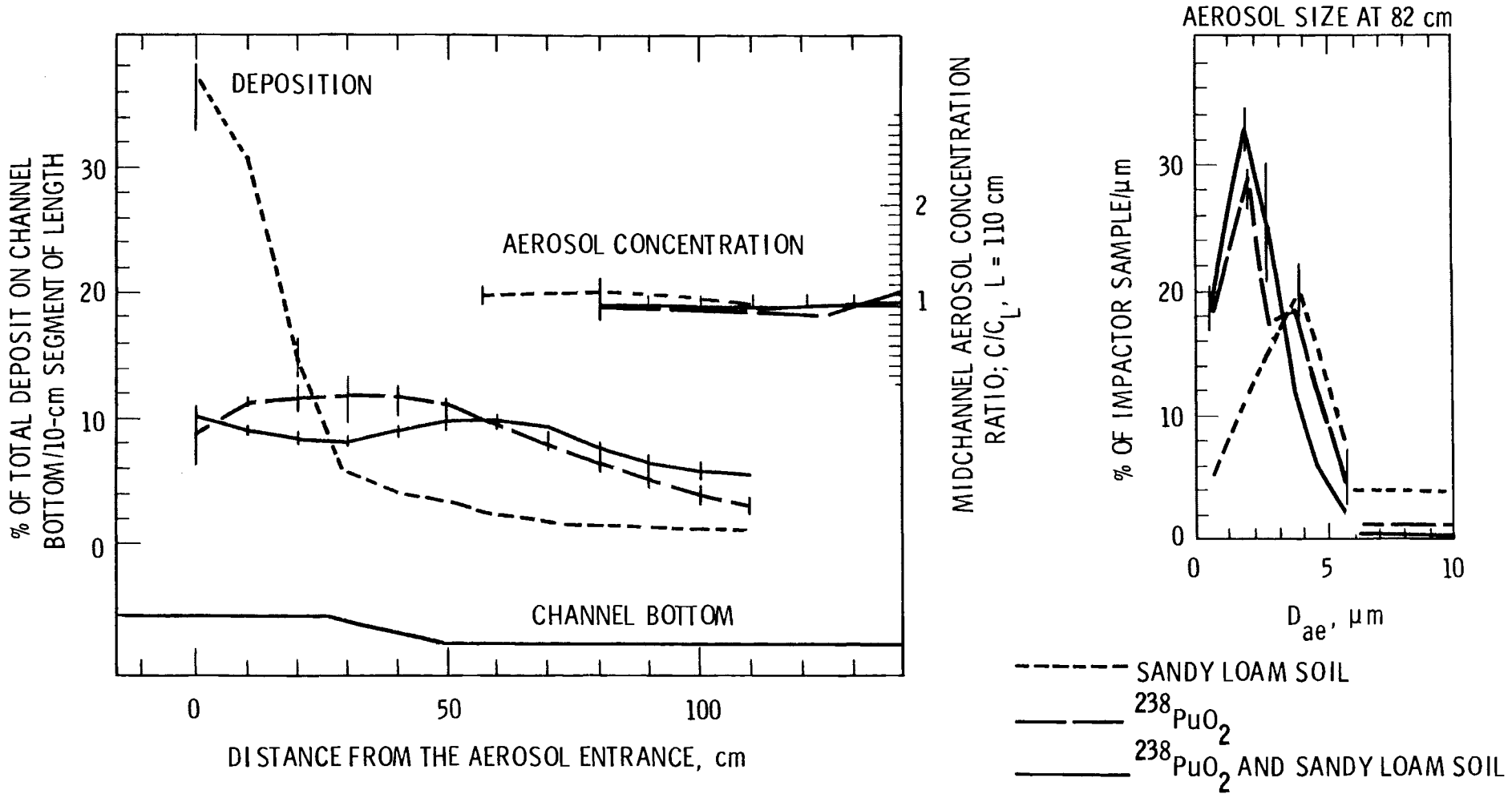

FIGURE 6. Deposition of Dust Along Length of Wind Tunnel for Sandy Loam Soil Plus $^{238}PuO_2$ Aerosols

SAMPLING: PARTICLE SIZE, D_p

The projected area diameter size distribution was obtained from electron micrographs similar to those shown in Figure 7. The $^{238}PuO_2$ aerosol had a bimodal, log-normal distribution when the aerosol was first generated alone (Figure 8, top graph). In the repeat run (Figure 8, bottom graph), only the distribution of large (CMD = 0.1 μm) particles was observed. The composition of the first size distribution was obtained by an iterative graphical fit to the data points. The fraction of the "total" distribution composed of particles from the "small" distribution was estimated, and the parameters (CMD and GSD) of the two log-normal distributions were calculated. The combined curve was plotted with the original EM data, and the process was repeated until a best-fit curve was obtained. The results of this curve-fitting process are shown in Figure 9 for the clay soil and $^{238}PuO_2$ aerosols, and in Figure 10 for the sandy loam soil and $^{238}PuO_2$ aerosols. The size distributions measured by this method are listed in Table 2.

SAMPLING: PARTICLE SIZE, AR SIZING

Bimodal, log-normal particle size distributions were seen for the $^{238}PuO_2$ aerosol and for the second run of each plutonium/soil aerosol mixture (Figure 11). The samples of aerosol taken during the first experiment of each series did not contain a noticeable distribution of small particles (curves 64-3 and 65-3, Figure 11). Autoradiography (AR) measured only the size distribution of $^{238}PuO_2$ particles; electron microscopy (EM) was used to size any particles present, regardless of composition. The size distributions measured for $^{238}PuO_2$ by EM and AR are presented together in Figure 12. The $^{238}PuO_2$ particle-size distribution, measured by EM for the repeat run (66-2A), agrees fairly well with the AR sizing from the first experiment (66-1), though the

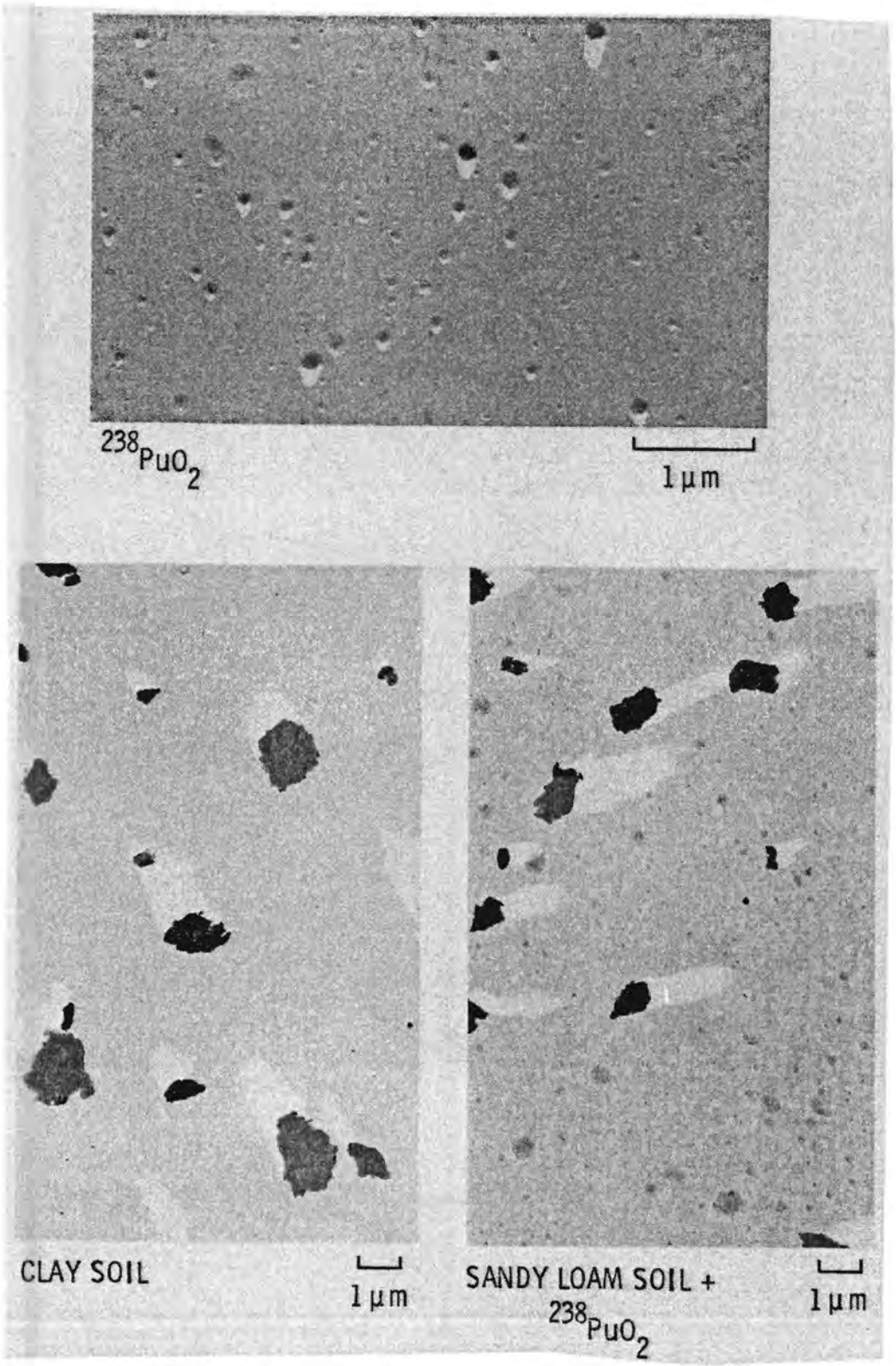

FIGURE 7. Electron Micrographs of Particles Sampled 100 cm from Aerosol Inlet

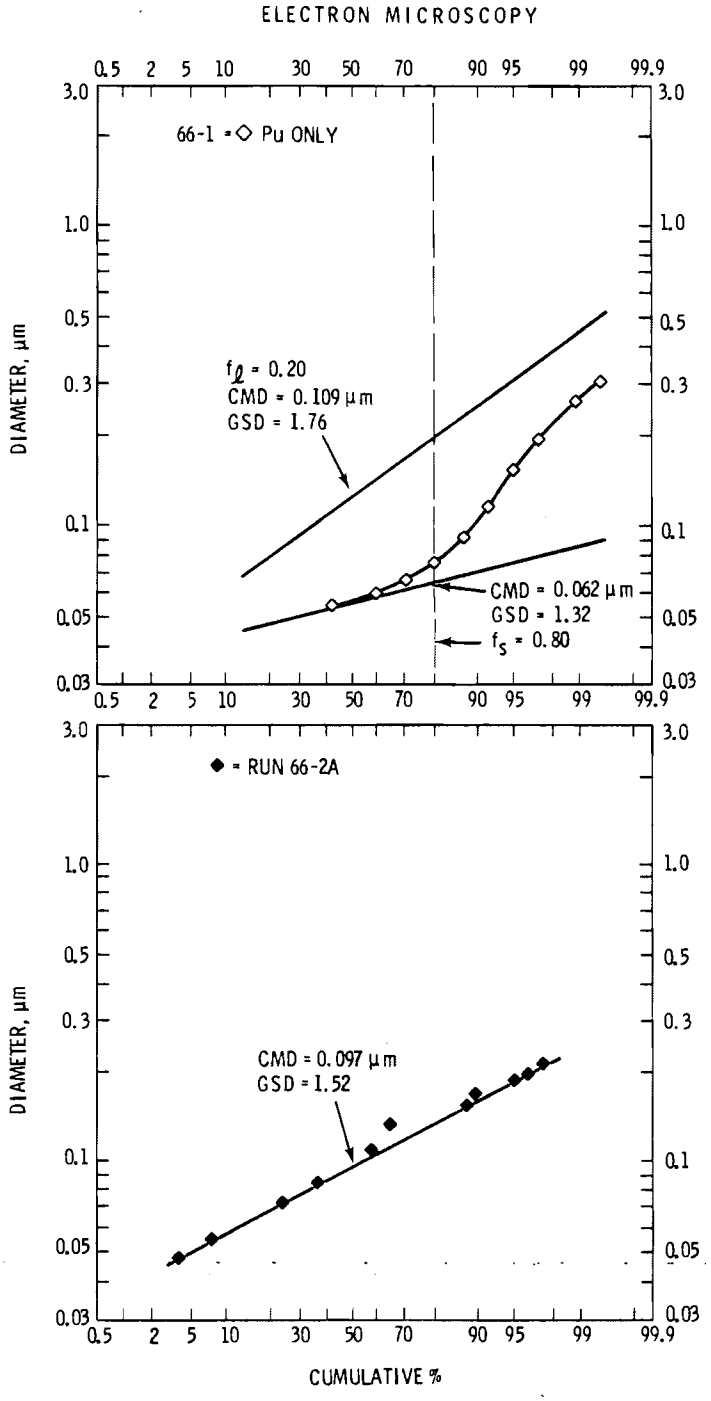

FIGURE 8. Particle Size Distribution Determined by Electron Microscopy for $^{238}PuO_2$ Aerosols

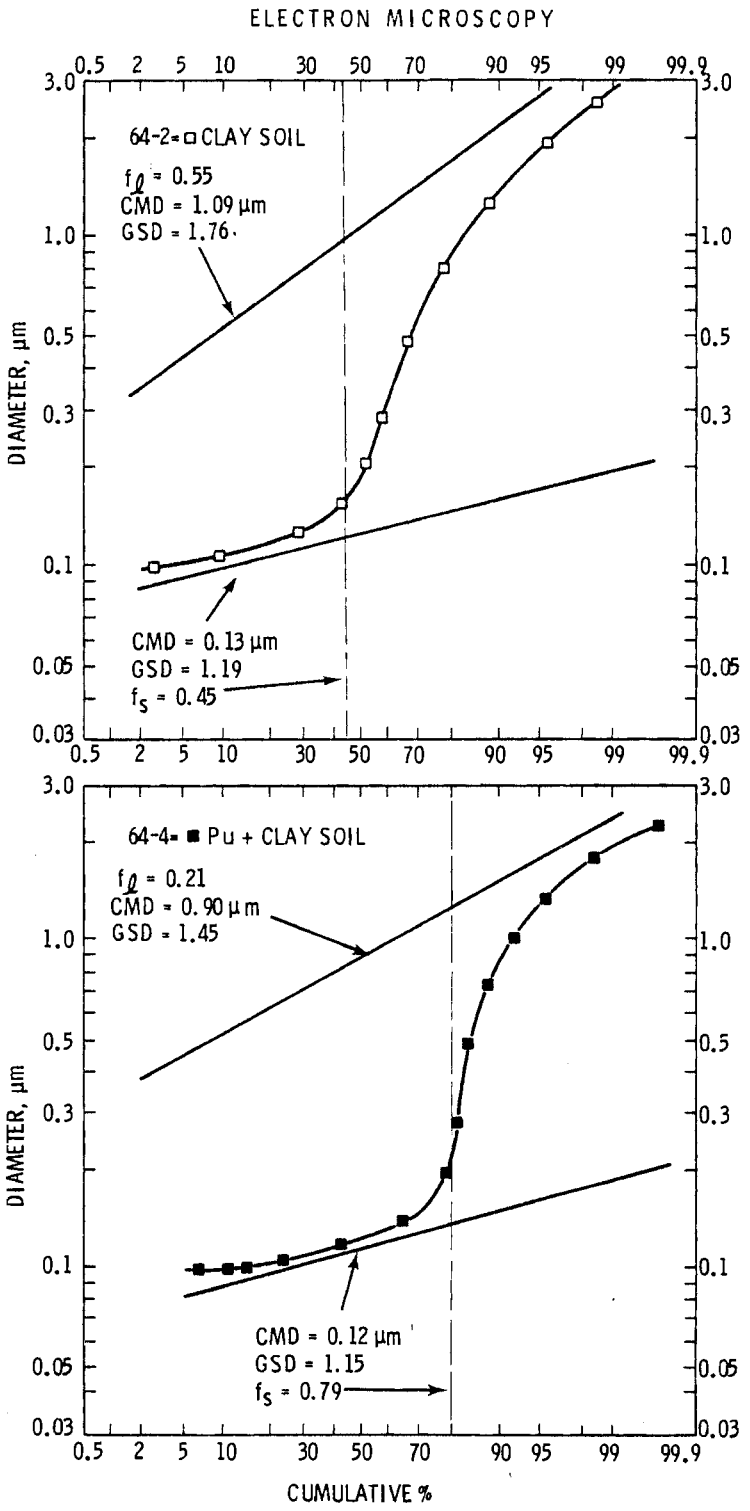

FIGURE 9. Particle Size Distribution Determined by Electron Microscopy for Clay Soil and $^{238}PuO_2$ Aerosols

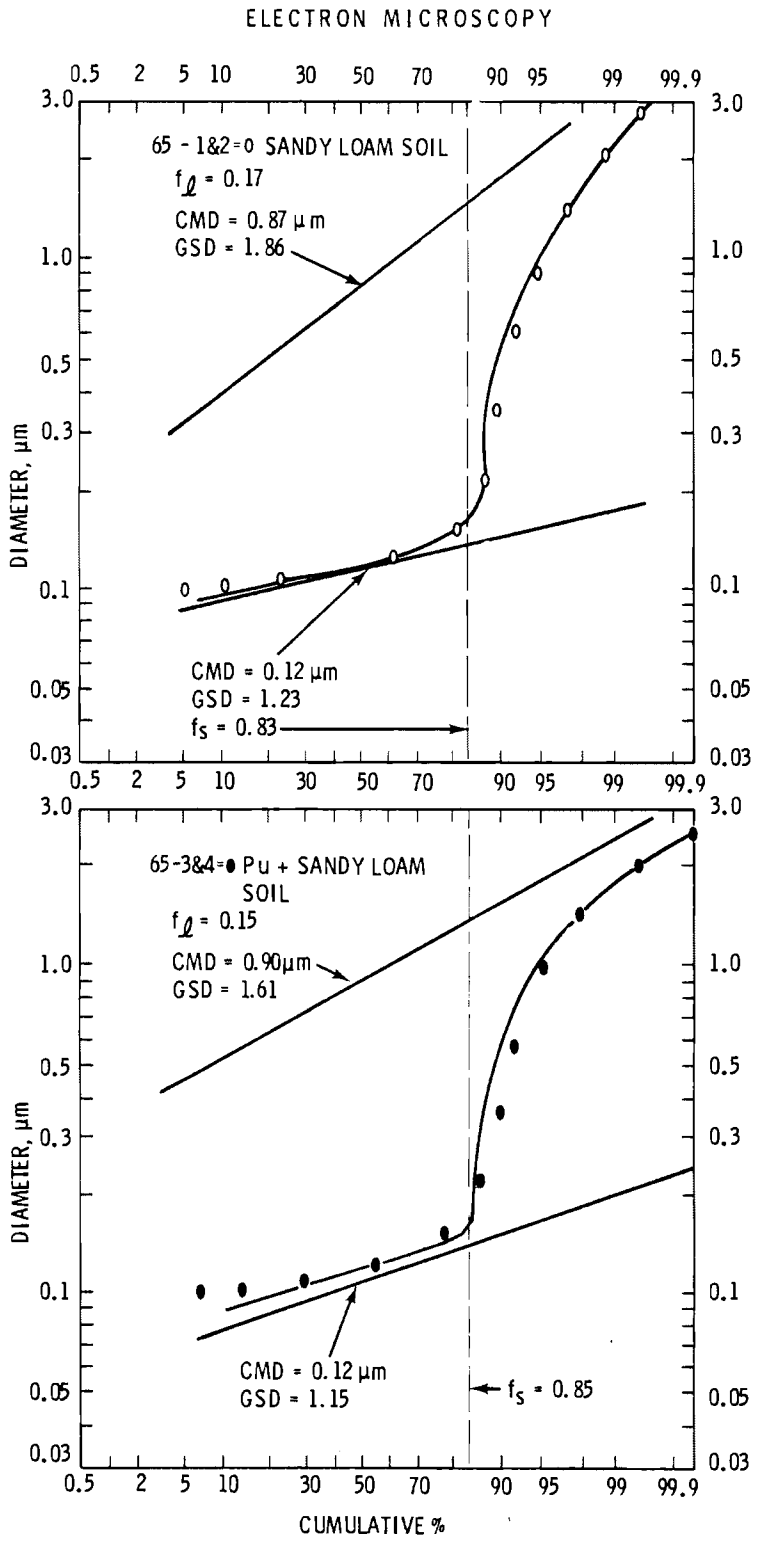

FIGURE 10. Particle Size Distribution Determined by Electron Microscopy for Sandy Loam Soil and $^{238}PuO_2$ Aerosols

TABLE 2. Projected Area Diameter Distribution of Particles Airborne at the End of the Wind Tunnel (100 cm from Inlet)

AEROSOL	SMALL PARTICLES, % OF TOTAL (BY COUNT)	COUNT DISTRIBUTION OF SMALL PARTICLES		COUNT DISTRIBUTION OF LARGE PARTICLES	
		CMD[a] µm	GSD[b]	CMD µm	GSD
CLAY SOIL	45	0.13	1.19	1.09	1.76
SANDY LOAM SOIL	83	0.12	1.23	0.87	1.86
$^{238}PuO_2$	80	0.062	1.32	0.11	1.76
$^{238}PuO_2$	0	--	--	0.10	1.52
$^{238}PuO_2$ + CLAY SOIL	79	0.12	1.15	0.90	1.45
$^{238}PuO_2$ + SANDY LOAM SOIL	85	0.12	1.15	0.90	1.61

[a] CMD = COUNT MEDIAN DIAMETER

[b] GSD = GEOMETRIC STANDARD DEVIATION

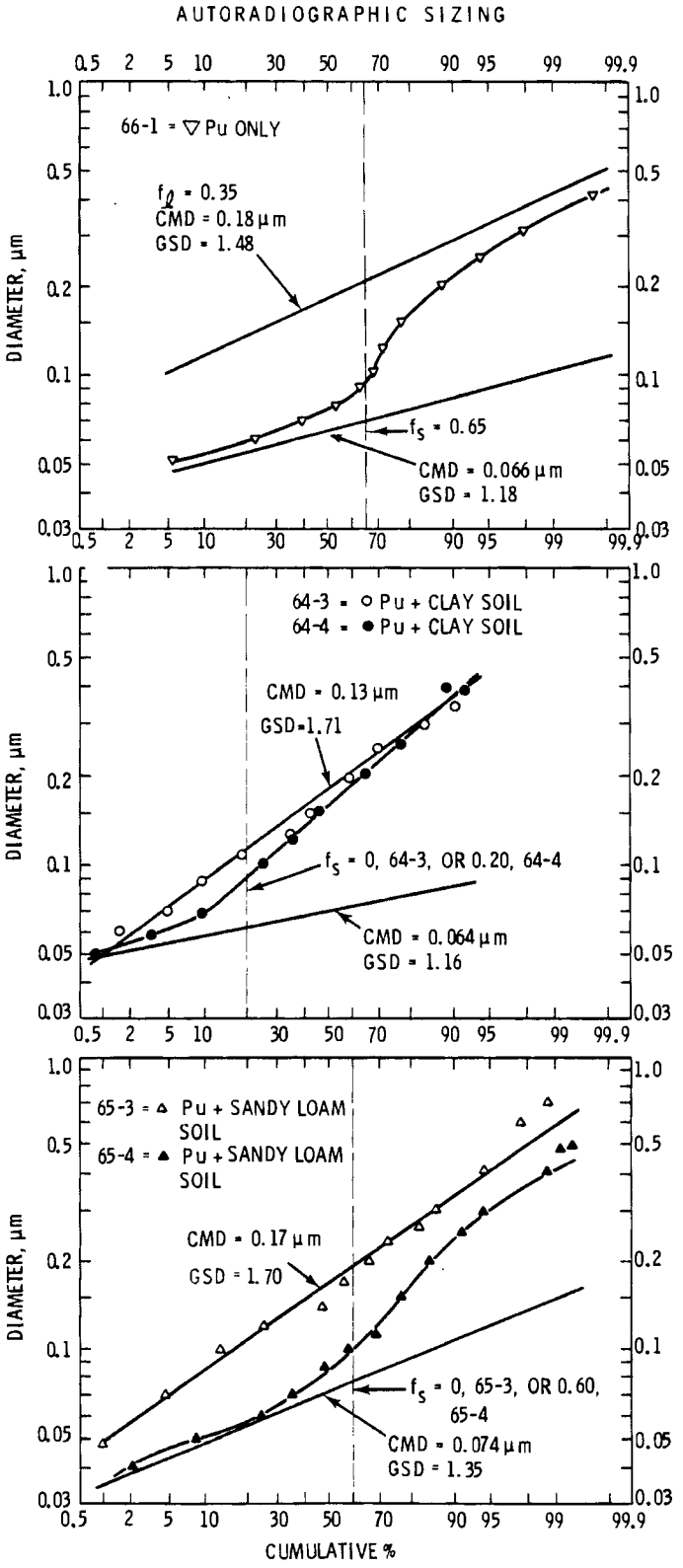

FIGURE 11. Particle Size Distribution Determined by Autoradiography for Plutonium/Soil Aerosol Mixture

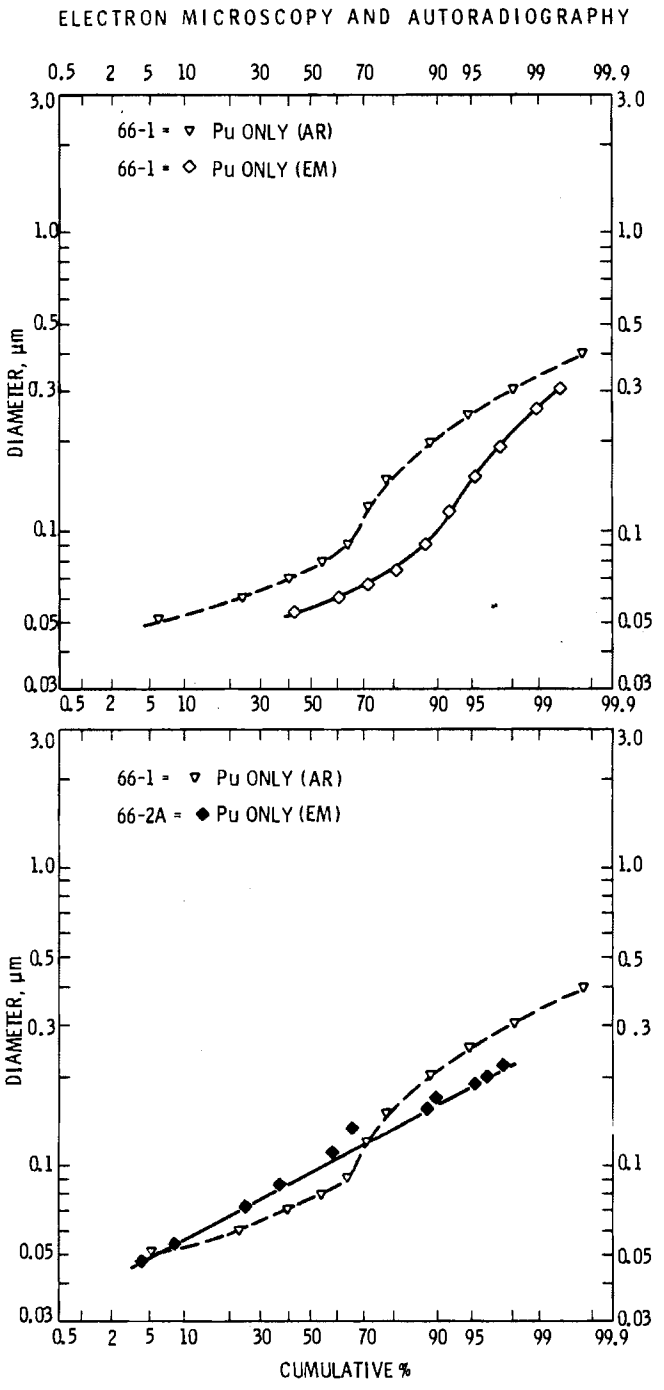

FIGURE 12. Particle Size Distribution for $^{238}PuO_2$ Aerosol Measured by Electron Microscopy and Autoradiography

EM data was fit with a single log-normal curve. The AR and EM data collected for $^{238}PuO_2$ on the same experimental run differ mainly in the percentage of small particles present (Tables 2 and 3, Figure 12): The sample measured by EM contained 80% (vs 65%) small particles. The difference, which is marginal, would be expected for a sample taken twice as far from the aerosol entrance into the wind tunnel.

The EM sizing technique measures all particles sampled; the AR sizing technique detects only the plutonium particles present. The AR technique should show the change in the plutonium aerosol when generated in the presence of a soil aerosol. The EM technique should show the presence of an additional size distribution of particles when a soil aerosol and plutonium aerosol are generated together. In Figure 13, these shifts are seen for the clay soil experiments (Figure 13, top graph). The airborne distribution of small particles decreases from 65% to 20% or 0 when $^{238}PuO_2$ is generated with a clay soil aerosol (Table 3). The presence of the $^{238}PuO_2$ distribution is detected in the EM samples by the increase in the percentage of small particles from 45 to 79% (Table 2). Only slight changes were observed in the particle-size distribution of the sandy loam soil aerosol in the presence of the $^{238}PuO_2$ aerosol and in the particle-size distribution of the $^{238}PuO_2$ aerosol in the presence of the sandy loam soil aerosol (Figure 13, bottom graph).

TABLE 3. Autoradiographic Measurement of the Particile Size Distribution Sampled at 57 cm From The Inlet of the Wind Tunnel

AEROSOL	$^{238}PuO_2$ PARTICLE SIZING: SMALL PARTICLES % OF TOTAL (BY COUNT)	COUNT DISTRIBUTION OF SMALL PARTICLES: CMD [b] µm	GSD [c]	COUNT DISTRIBUTION OF LARGE PARTICLES: CMD µm	GSD	SOIL PARTICLE SIZING [a]: TOTAL NUMBER OF PARTICLES SIZED	% OF THE PARTICLES IN EACH SIZE INTERVAL: <0.9µm	0.9µm-2.2µm	>2.2µm
$^{238}PuO_2$	65	0.066	1.18	0.18	1.48	--	--	--	--
$^{238}PuO_2$ + CLAY SOIL	0	--	--	0.13	1.71	--	--	--	--
	20	0.064	1.16	0.13	1.71	200	77	14	9
$^{238}PuO_2$ + SANDY LOAM SOIL	0	--	--	0.17	1.70	--	--	--	--
	60	0.074	1.35	0.17	1.70	236	76	16	8

[a] FROM LIGHT MICROSCOPY OF THE SOIL PARTICLES ASSOCIATED WITH SOME OF THE PLUTONIUM PARTICLES

[b] CMD = COUNT MEDIAN DIAMETER

[c] GSD = GEOMETRIC STANDARD DEVIATION

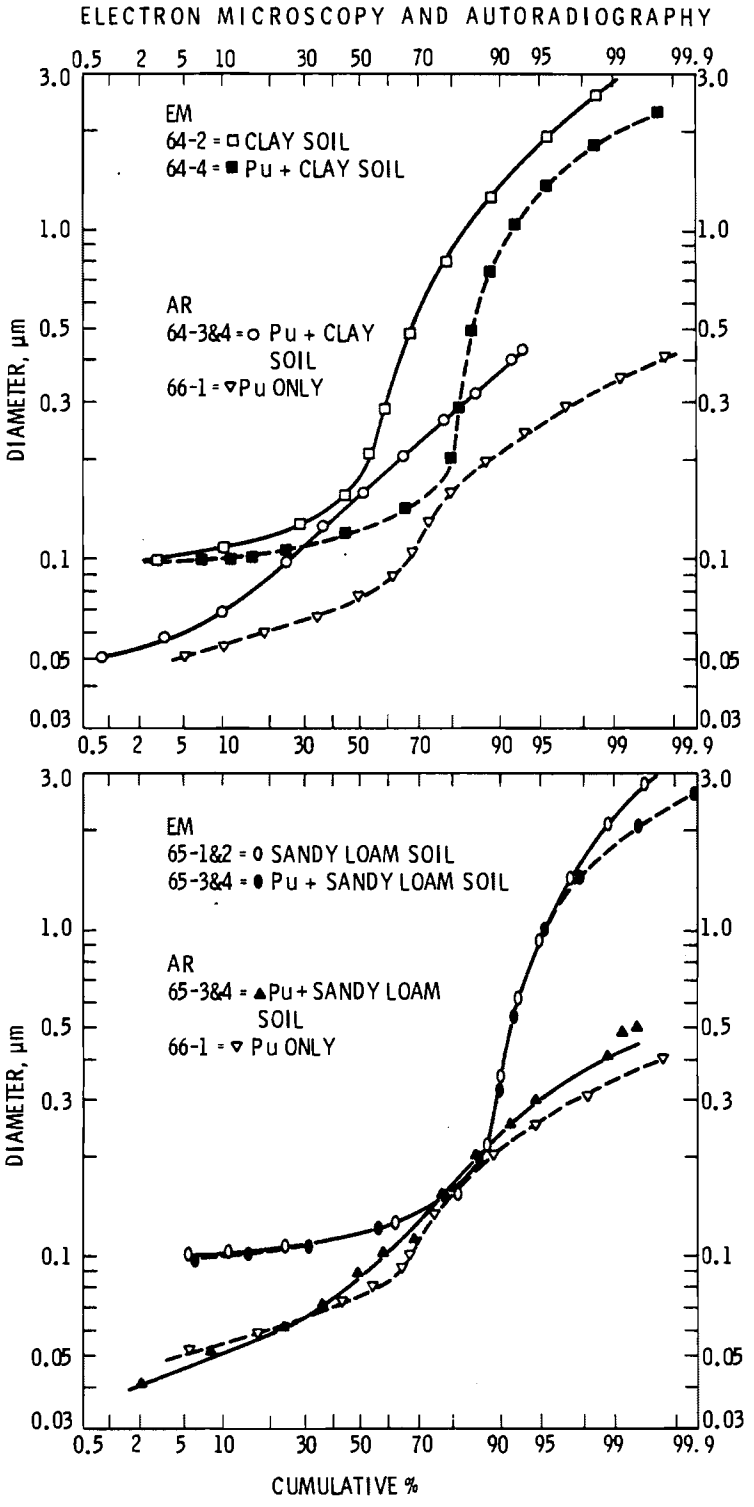

FIGURE 13. Airborne Distribution by Electron Microscopy and Autoradiography for Clay Soil, Sandy Loam Soil and $^{238}PuO_2$ Aerosols

DISCUSSION

The individual aerosols ($^{238}PuO_2$, clay soil and sandy loam soil) differed in size distribution and in the percentage of material airborne at 110 cm from the aerosol entrance. Of the total mass generated as an aerosol, 15% of the clay soil and 4% of the sandy loam soil remained airborne at the end of the wind tunnel. The sandy loam soil contained more large particles than the clay soil aerosol. The size distribution of the $^{238}PuO_2$ aerosol was much smaller than that of either soil aerosol: 84% of the total activity that was generated remained airborne at the end of the wind tunnel. These differences among the three aerosols were reflected in all of the subsequent measurements and comparisons.

Differences between plutonium aerosol generated with the clay soil aerosol and that generated alone were:

- Airborne mass 110 cm down the wind tunnel increased slightly: 3 to 12% (Table 1, Figure 5).
- Aerodynamic size distribution of airborne material 82 cm down the wind tunnel remained approximately the same. Geometric standard deviation decreased slightly: 2.5 to 2.3 (Table 1).
- Bimodal particle count distribution changed, based on autoradiographic sizing. The distribution of large particles increased in relative number from 35% to 80%. The count median diameter increased from 1.4 to 1.7 (Tables 2 and 3, Figures 11 and 13).
- The presence of plutonium particles was detected as a shift in the count distribution measured by EM (Figure 13, Table 2).

- At 82 cm down the wind tunnel, airborne particle number concentration decreased. There were 49% fewer $^{238}PuO_2$ particles airborne at the sampling point when the clay soil aerosol was generated with the $^{238}PuO_2$ (Table 4, last column, "normalized C_n"). To obtain these numbers, the diameter of the particle of average volume, $\bar{D}_v$, was calculated from the AMAD. In Table 4, C_n was corrected for the fact that the initial concentration of $^{238}PuO_2$ in the nebulizer solution was not the same in all experiments (Table 1, column 2).

The changes seen in the plutonium aerosol when it was generated with the sandy loam soil were:

- Airborne activity 110 cm down the wind tunnel decreased slightly: approximately 5% (Table 1, Figure 6).
- At 82 cm down the wind tunnel, aerodynamic size distribution decreased in AMAD (2.1 vs 1.8), and in GSD (2.5 vs 2.2; Table 1).
- Based on autoradiographic sizing on samples collected at 57 cm down the wind tunnel, bimodal particle count distribution remained approximately the same (Table 3).
- No change was observed in the count distribution measured by EM (Figure 13, Table 2).
- At 82 cm down the tunnel, particle count decreased: 65% fewer particles (Table 4).

TABLE 4. Calculations of Airborne Particle Concentration 82 cm from Inlet

AEROSOL	AMAD μm	GSD	AIRBORNE CONCENTRATION [a,b]	C_n [c] PARTICLES/cm^3	NORMALIZED C_n [d] PARTICLES/cm^3
CLAY SOIL	2.85 ± 0.05[a]	2.25 ± 0.05[a]	168 ± 22 μg/ℓ	$5.0 \times 10^{+5}$	--
SANDY LOAM SOIL	4.1 ± 0	2.45 ± 0.05	58 ± 0.5 μg/ℓ	$1.2 \times 10^{+5}$	--
$^{238}PuO_2$	2.1 ± 0.1	2.5 ± 0	1049 ± 107 nCi/ℓ	$8.7 \times 10^{+3}$	8,700
$^{238}PuO_2$ + CLAY SOIL	2.1 ± 0.2	2.3 ± 0.1	763 ± 37 nCi/ℓ	$2.8 \times 10^{+3}$	4,400
$^{238}PuO_2$ + SANDY LOAM SOIL	2.0 ± 0.2	2.15 ± 0.05	490 ± 10 nCi/ℓ	$1.5 \times 10^{+3}$	3,120

[a] AVERAGE ± 1/2 THE DIFFERENCE BETWEEN THE TWO EXPERIMENTS

[b] AIRBORNE ACTIVITY SAMPLED AT 110 cm IS THE SAME AS THAT SAMPLED AT 82 cm. THE CONCENTRATION WAS MEASURED AT 110 cm (TABLE 1).

[c] ESTIMATED PuO_2 PARTICLE CONCENTRATION IN THE WIND TUNNEL

[d] NORMALIZED TO THE TOTAL AMOUNT GENERATED BASED ON MEASUREMENTS IN THE WIND TUNNEL

SUMMARY

These five experiments demonstrate that at initial concentrations of soil and plutonium dioxide of 0.6 to 2.5 x 10^6 and 0.04 x 10^6 particles/cm^3, respectively, the presence of a soil aerosol caused a change in the airborne source term. The following changes were observed:

- total activity concentration decreased by 5%;
- particle count decreased by 65 and 49%, respectively;
- the spread in particle size distribution decreased;
- no significant change was seen in the respirable fraction.

The theoretical model for Brownian coagulation predicted that there would be no measurable change in the aerodynamic size distribution of the $^{238}PuO_2$ due to the presence of the soil aerosol at the concentrations used in these experiments. The changes seen in these experiments show the influence of particle scavenging due to sedimentation of soil particles through a cloud of $^{238}PuO_2$ aerosol. This is assumed to be the dominant mechanism for reducing the respirable PuO_2 aerosol concentration for the period between a few seconds and a few minutes following impact. The major reduction in the source term is expected to occur in the first few seconds due to Brownian and turbulent coagulation; however, these processes are important only at high particle concentrations, and were therefore not tested in these experiments. For the theoretical model assumed in this report, the respirable PuO_2 aerosol concentration was predicted to decrease from 10^6 to 10^4 particles/cm^3 due to Brownian coagulation.

REFERENCES

1. Craig, D. K., Cannon, W. C., Filipy, R. E., Mahlum, D. D., and Smith, V. H. (1974). "SNS Source Term Evaluation Program, Annual Report." BNWL-1856, Pacific Northwest Laboratory, Richland, WA.

2. Moore, H. J. (1976). "Missile Impact Craters (White Sands Missile Range, New Mexico) and Applications to Lunar Research." Contributions to Astrogeology, Geological Survey Professional Paper 812-B, U. S. Government Printing Office, Washington, DC.

3. NUS Corporation. (1974). "Overall Safety Manual," Vol. IV, pp. 53-56 (for USAEC, Space Nuclear Systems Division, Contract SNSO-7). NUS Corporation, Rockville, MD.

4. Ibid., Vol. II, pp. 2.8-6.

5. Ibid., Vol. II, pp. 2.8-33.

6. Mercer, T. T. (1973). Aerosol Technology in Hazard Evaluation, p. 96. Academic Press, New York.

7. NUS Corporation. (1974). "Overall Safety Manual," Vol. IV, p. 47 (for USAEC, Space Nuclear Systems Division, Contract SNSO-7). NUS Corporation, Rockville, MD.

8. Mercer, T. T. (1973). Aerosol Technology in Hazard Evaluation, pp. 45-48. Academic Press, New York.

9. Mercer, T. T. (1978). Chapter 2, Brownian Coagulation: Experimental Methods and Results, pp. 85-131. In: Fundamentals of Aerosol Science, Shaw, D. T. (ed.). John Wiley & Sons, New York.

10. Pitch, J. (1972). A mathematical study of the Wiegner effect in colloid coagulation, pp. 5-17. In: Assessment of Airborne Particles, Mercer, T. T., Morrow, P. E., Stober, W. (eds.), Charles C. Thomas, Springfield, IL.

11. Greenfield, M. A., Koontz, R. L., and Hausknecht, D. F. (1971). Comparison of experiment and theory for the coagulation of aerosols. J. Colloid Interface Sci. 35(1): 102-113.

12. Zebel, G. (1966). Chapter II, Coagulation of Aerosols, pp. 31-58. In: Aerosol Science, Davies, C. N. (ed.). Academic Press, New York.

13. von Smoluchowski, M. (1917). A mathematical theory of the kinetics of coagulation of colloidal solutions. Z. Phys. Chem. 92: 129-168.

14. Friedlander, S. K. (1977). Smoke, Dust, and Haze: Fundamentals of Aerosol Behavior. John Wiley and Sons, New York.

15. Craig, D. K., Klepper, B. L., and Buschbom, R. L. (1974). Deposition of Various Plutonium-Compound Aerosols onto Plant Foliage at Very Low Wind Velocities, pp. 244-263. In: "Atmosphere-Surface Exchange of Particulate and Gaseous Pollutants." CONF-740921, NTIS, Springfield, VA.

16. Craig, D. K. and Klepper, B. L. (1975). The design and calibration of a low speed windtunnel for studying the foliar deposition and uptake of aerosol. Am. Ind. Hyg. Assoc. J. 36: 692-699.

17. Wright, B. M. (1950). A new dust-feed mechanism. J. Sci. Instrum. 27: 12-15.

18. Craig, D. K., Cannon, W. C., Filipy, R. E., Powers, G. J., and Dionne, P. J. (1976). "SNS Source Term Evaluation Program, Annual Report," p. 44. BNWL-1971, Pacific Northwest Laboratory, Richland, WA.

19. Moss, O. R., Filipy, R. E., Cannon, W. C., and Craig, D. K. (1977). SNS Source Term Evaluation Program, Annual Report." BNWL-2255, Pacific Northwest Laboratory, Richland, WA (in press).

20. Swift, D. L. (1978). Thermal Precipitators, pp. Q1-Q10. In: "Air Sampling Instruments, 5th Edition." American Conference of Governmental Industrial Hygienists, Cinicinnati, OH.

DISTRIBUTION

No. of Copies

OFFSITE

A. A. Churm
DOE Patent Division
9800 South Cass Avenue
Argonne, Il 60439

27 DOE Technical Information Center

Dr. William Ailor
The Aerospace Corporation
P. O. Box 92957
Los Angeles, CA 90009

Denton C. Anderson
Teledyne Energy Systems
110 W. Timonium Road
Timonium, MD 21093

C. M. Barnes
L. B. Johnson Space Center
NASA, SPS
Houston, TX 77058

Harold Battaglia
L.B. Johnson Space Center
NASA, PF
Houston, TX 77058

Maj Randall E. Beatty
HQ AFSC/IGF
Andrews AFB, D.C. 20334

Dr. G. L. Bennett
U.S. Department of Energy
Mail Station B-107
Washington, D.C. 20545

W. H. Boggs
J. F. Kennedy Space Center
NASA, DE-A
Kennedy Space Center, FL 32899

C. T. Bradshaw
General Electric Co.
P.O. Box 8661
Philadelphia, PA 19101

No. of Copies

S. E. Bronisz
Los Alamos Scientific Lab
P. O. Box 1663
Los Alamos, NM 87545

R. H. Brown
L. B. Johnson Space Center
NASA, FM
Houston, TX 77058

R. A. Brownback
Savannah River Plant
E. I. duPont de Nemours and Company
Aiken, SC 29808

R. C. Campbell
Jet Propulsion Laboratory
4800 Oak Grove Drive
Pasadena, CA 91103

T. Carter
Nuclear Regulatory Commission
NMSS
Washington, D.C. 20555

John Casani
Jet Propulsion Laboratory
Mail Code 169-427
4800 Oak Grove Drive
Pasadena, CA 91103

C. R. Chappell
Nuclear Regulatory Commission
Mail Stop 396-SS
Washington, D.C. 20555

Maj Emery Chase
ATSD/AE
Washington, D.C. 20301

Victor Christensen, MD - ESB
J. F. Kennedy Space Center
NASA, MD-E
Kennedy Space Center, FL 32899

No. of
Copies

Lt Nicolas Clemens
AFWL/DYDS
Kirtland AFB, NM 87117

R. S. Coffey
NUS Corporation
4 Research Place
Rockville, MD 20850

Roy H. Cooper
Metals and Ceramics Division
Oak Ridge National Laboratory
P.O. Box X
Oak Ridge, TN 37830

R. Corridan
Ames Research Center
NASA
Moffett Field, CA 94035

J. P. Crane
U.S. Department of Energy
Albuquerque Operations Office
P. O. Box 5400
Albuquerque, NM 87115

Maj Dave Daniels
HQ AFSC/IGF
Andrews AFB, D.C. 20334

G. P. Dix
U.S. Department of Energy
Mail Station E-201
Washington, D. C. 20545

T. J. Dobry
U.S. Department of Energy
Mail Station E-201
Washington, D.C. 20545

Lt Catherine J. Dower
AFWL/DYVS
Kirtland AFB, NM 87117

D. Egan
Office of Radiation Programs
(ANR-460)
USEPA
Washington, D.C. 20460

No. of
Copies

Ken Elliot
U.S. Department of Energy
Operational Safety Division
Albuquerque Operations Office
P. O. Box 5400
Albuquerque, NM 87115

R. W. Englehart
NUS Corporation
4 Research Place
Rockville, MD 20850

Lt John Erb
ESMC SGPH
Patrick AFB, FL 32925

R. L. Folger
Savannah River Laboratory
E. I. duPont de Nemours
and Company
Aiken, SC 29808

Dr. Ralph R. Fullwood
Science Applications, Inc.
5 Palo Alto Square
Suite 200
Palo Alto, CA 94304

Ed Gabris
NASA HQ
RST-5
Washington, D.C. 20546

J. J. Givens
Ames Research Center
NASA
Moffett Field, CA 94035

Don Glenn
The Aerospace Corporation
P.O. Box 92957
Los Angeles, CA 90009

Dr. Marvin Goldman
Professor of Radiobiology
Radiobiology Laboratory
University of California
Davis, CA 95616

No. of Copies

W. T. Goldston, Jr.
U.S. Department of Energy
Savannah River Operations
Post Office Box A
Aiken, SC 29801

J. C. Hagan
Applied Physics Lab/JHU
John Hopkins Road
Laurel, MD 20810

D. S. Hess
Jet Propulsion Laboratory
4800 Oak Grove Drive
Pasadena, CA 91103

2 Lt Jeffrey W. Hess
AFWL/DYVS
Kirtland AFB, NM 87117

R. G. Ivanoff
Jet Propulsion Laboratory
4800 Oak Grove Drive
Pasadena, CA 91103

E. W. Johnson
Monsanto Research Corporation
Mound Laboratory
P.O. Box 32
Miamisburg, OH 45342

T. Kerr
NASA HQ
DS-3
Washington, D.C. 20546

Dr. William Kessler
AFML/MPE
Wright-Patterson AFB, OH 45433

D. Krenz
U.S. Department of Energy
Albuquerque Operations Office
P. O. Box 5400
Albuquerque, NM 87115

J. J. Lombardo
U. S. Department of Energy
Mail Station B-107
Washington, D.C. 20545

No. of Copies

John Marshall
AFRPL/LKC
Edwards AFB, CA 93523

B. R. McCullar
NASA HQ
SL-4
Washington, D.C. 20546

M. McDonald
NASA HQ
ST-5
Washington, D.C. 20546

L. C. Montgomery
Jet Propulsion Laboratory
4800 Oak Grove Drive
Pasadena, CA 91103

Lt Col Ken Morrison
AFISC/SES
Norton AFB, CA 92409

Lt Col William B. Moyer
AFMSC/SGPZ
Brooks AFB, TX 78235

Lt Col Mel Nosal
AFISC/SES
Norton AFB, CA 92409

G. H. Ogburn
U.S. Department of Energy
Mail Station B-107
Washington, D.C. 20545

Operations and Systems Requirements
Code OP-6
NASA HQ
Washington, D.C. 20546

Dr. C. Osterberg
U.S. Department of Energy
Mail Station E-201
Washington, D.C. 20545

2 John A. Palmer
DET 1, AFISC/SNS
Kirtland AFB, NM 87117

No. of
Copies

L. M. Papouchado
Savannah River Plant
E. I. duPont de Nemours
and Company
Aiken, SC 29808

Lloyd Parker - SF
John F. Kennedy Space Center
NASA, SF
Kennedy Space Center, FL 32899

Joe Pidkowicz
U.S. Department of Energy
Oak Ridge Operations Office
P.O. Box E
Oak Ridge, TN 37830

W. C. Pitts
NASA, STPM
Ames Research Center
Moffett Field, CA 94035

W. I. Purdy, Jr.
Jet Propulsion Laboratory
4800 Oak Grove Drive
Pasadena, CA 91103

W. A. Riehl
Marshall Space Flight Center
NASA, EH 31
Marshall SFC, AL 35812

Bill Riley
WSMC/SE
Vandenburg AFB, CA 93437

J. C. Robinson
Langley Research Center
NASA, MS 395
Hampton, VA 23665

Ralph Robinson
AFWL/DYDS
Kirtland AFB, NM 87117

J. R. Roeder
U.S. Department of Energy
Albuquerque Operations Office
P. O. Box 5400
Albuquerque, NM 87115

No. of
Copies

R. G. Rose
L. B. Johnson Space Center
NASA, FA
Houston, TX 77058

G. J. Schaefer, Jr.
Lewis Research Center
NASA, MAIC 500-120
21000 Brookpark Road
Cleveland, OH 44135

J. A. Schellar
NASA HQ
MB-6
Washington, D.C. 20546

F. R. Schmidt
NASA HQ
OLE-9
Washington, D.C. 20546

Maj Terry Schmidt
AFWL/NTYV
Kirtland AFB, NM 87117

Norman Schulze
NASA HQ
MHR-7
Washington, D.C. 20546

Lt Michael K. Seaton
AFWL/DYVS
Kirtland AFB, NM 87117

L. T. Shaw
Jet Propulsion Laboratory
4800 Oak Grove Drive
Pasadena, CA 91103

Capt Charles Snow
SAMSO/SE
P.O. Box 92960
Worldway Postal Center
Los Angeles, CA 90009

No. of
Copies

R. J. Spehalski
Jet Propulsion Laboratory
4800 Oak Grove Drive
Pasadena, CA 91103

R. C. Turkolu
TRW
Defense and Space Systems Group
One Space Park
Redondo Beach, CA 90278

Lou J. Ullian, Chairman
ESMC/SE
Patrick AFB, FL 32925

Dr. I. Van Der Hoven
U.S. Department of Energy
Mail Station B-107
Washington, D.C. 20545

G. R. Waterbury
Los Alamos Scientific Lab
P. O. Box 1663
Los Alamos, NM 87545

Maj Walt Wilson
AFISC/SEM
Norton AFB, CA 92409

Maj R. O. Winchester
Det 1, AFISC
Kirtland AFB, NM 87117

J. A. Yoder
U.S. Department of Energy
Mail Station E-201
Washington, D.C. 20545

Lt Douglas Zimmerman
AFWAL/MLBE
Wright-Patterson AFB, OH 45433

ONSITE

2 DOE Richland Operations Office

R. K. Stewart
H. E. Ransom

No. of
Copies

29 Pacific NW Laboratory

W. J. Bair
W. C. Cannon (2)
H. Drucker
R. E. Filipy (2)
M. T. Karagianes
O. R. Moss (5)
E. J. Rossignol
G. A. Sehmel
R. C. Thompson
R. E. Wildung
W. R. Wiley
Biology Library (2)
Technical Information
Files (5)
Publishing Coordination (2)